H. Talja, H. Kordisch†, and L. Hodulak†*

Assessment of Stable Growth of Surface Flaws

REFERENCE Talja, H., Kordisch, H., and Hodulak, L., **Assessment of stable growth of surface flaws**, *Defect Assessment in Components – Fundamentals and Applications*, ESIS/EGF9 (Edited by J. G. Blauel and K.-H. Schwalbe) 1991, Mechanical Engineering Publications, London, pp. 1025–1039.

ABSTRACT Safety assessments of flawed structures are normally based on fracture mechanics parameter values measured from small specimens. The transferability of those results is not yet completely assured because small specimens under simple loads may behave in a different way from real structures in complex loading situations.

As a step in improving the accuracy of numerical simulation of stable crack growth, a method has been developed at Fh-IWM to take the constraint dependence of the crack growth resistance along crack front into account. In order to verify the method a large flawed steel plate was tested under four point bending. Fracture resistance curves were measured from a number of CT specimens. The fracture behaviour of the plate was assessed with analytical methods and with the finite element method. The three-dimensional finite element calculations contained stationary analyses and simulations of stable crack growth with unique and constraint dependent fracture resistance curves. The analytical methods proved to give realistic, conservative results. Stationary FE calculations overestimated crack growth. Best agreement between calculation and experiment was obtained when the new method was used.

Introduction

Advanced methods to assess the behaviour of surface flaws in ductile materials are necessary in safety assessments, for instance in leak before break considerations. But the transferability of experimental results from small specimens to real components and structures, however, is not yet completely assured for several reasons.

(1) The local loading conditions can vary strongly along the crack front as indicated by J calculations and three-dimensional elastic–plastic calculation methods are necessary to obtain good results.
(2) The material resistance against crack growth varies along the crack front even in homogeneous materials due to the variation of the local triaxiality of the stress state. Due to this 'constraint effect', the J_R curves measured from smooth or side-grooved specimens or specimens with different geometries and dimensions are different.
(3) The crack growth resistance curves are measured at constant temperature using mechanical loadings. The real loading situation can be very complex, for example the temperature gradient load due to emergency cooling of a reactor pressure vessel (RPV).

* Technical Research Centre of Finland (VTT), Nuclear Engineering Laboratory, PO Box 169, SF-00181 Helsinki, Finland.
† Fraunhofer-Institut für Werkstoffmechanik (Fh. IWM), Wöhlerstraße 11, D-7800 Freiburg, FRG.

(4) The use of a lower bound J_R curve obtained from side-grooved specimens may yield a wrong estimate of the development of the crack shape. This can lead to an overly conservative assessment when for instance the leak-before-break behaviour is considered.

Extensive verification is necessary before new methods can be adopted in practical safety assessments. This study is intended to be a part of such validation work.

Model for consideration of stress state

In order to take account of the difficulties in the assessment of stable crack growth mentioned above, at Fh-IWM a method has recently been developed, based on the simplifying assumption that the local initiation and growth of cracks depend on the local value of the loading parameter and the local fracture resistance, influenced by the local triaxiality of the stress strain state (3). The degree of the triaxiality is described by a constraint factor h defined as

$$h = \sigma_h/\sigma_v$$

quotient of the mean or hydrostatic stress σ_h to the equivalent stress σ_v after von Mises. To describe the geometry effect, the average value of the constraint factor h_m as calculated ahead of the crack front of the corresponding CT specimen is correlated to the measured J_R curve. This is consistent with the fact that a J_R curve essentially represents the dependence between average J integral and average crack growth. For smooth or side-grooved CT specimens with different slopes dJ/da, the h_m values are different.

In a first step a linear relationship between h_m and the slope dJ/da is established which is used to simulate the local crack growth of a crack in a component of the same material. Moreover it is assumed that the constraint effect does not influence the initiation value J_i.

Verification of the model

Description of experimental part

In order to verify the method and to get a supplementary link in the chain of transferability of results from small specimens to the assessment of pressurised thermal shock, a large flawed plate of the reactor pressure vessel steel 22 NiMoCr 37 was tested. The test was aimed as a preliminary study for the long-term pressurised thermal shock tests (THEL) in the German HDR reactor safety programme (5).

The plate test was performed under four point bending to obtain a stress gradient resembling to that in a RPV wall loaded by a pressurised thermal shock. Stable crack growth of a few millimetres was planned to be reached in the test. The test configuration is illustrated in Fig. 1. A semi-elliptical flaw was produced in the plate by machining and sharpened by fatigue. The depth

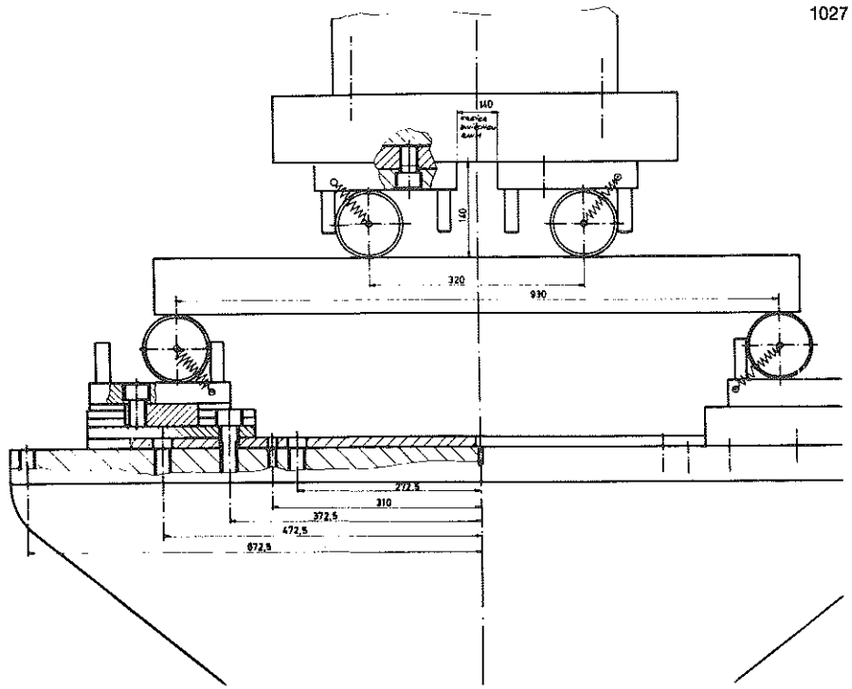

Fig 1 The configuration of the four point bending plate test

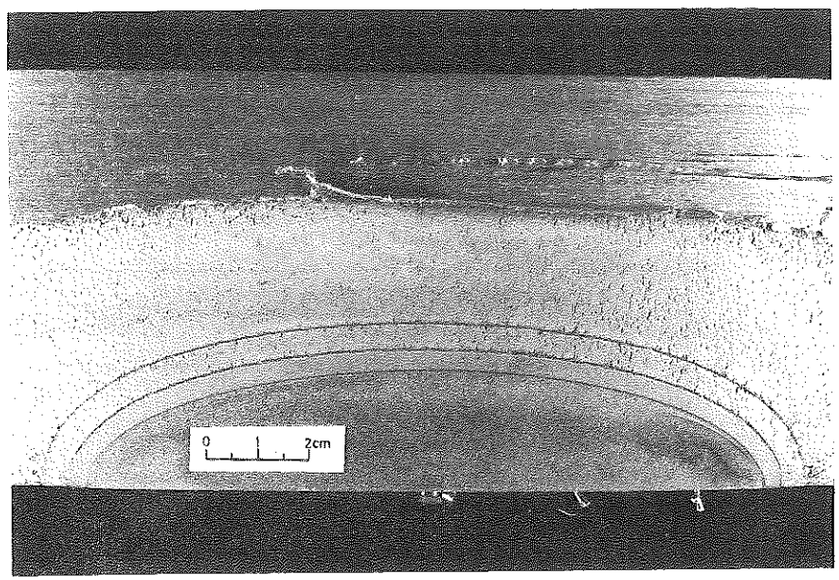

Fig 2 Fracture surface of the steel plate

a of the final surface flaw shown in Fig. 2 was 27.7 mm which is 35 percent of the thickness. The length $2c$ of the flaw was 140.4 mm ($a/c = 0.4$). The test was performed at a temperature of 70°C in order to assure upper shelf behaviour.

Stress–strain curves were defined for the material at test temperature. The yield stress was 443 MPa and the ultimate strength 572 MPa. J_R curves (shown in Fig. 3) were measured using the partial unloading compliance technique from smooth and side-grooved CT specimens of different dimensions (Table 1). Additionally, potential drop measurements were made to detect the initiation.

The plate was extensively instrumented. The values of load, load point displacement, and crack mouth opening displacement (CMOD) were measured during the test. Strain fields were measured with strain gauges to validate the numerical results. Acoustic emission measurements were made to detect the initiation of crack growth.

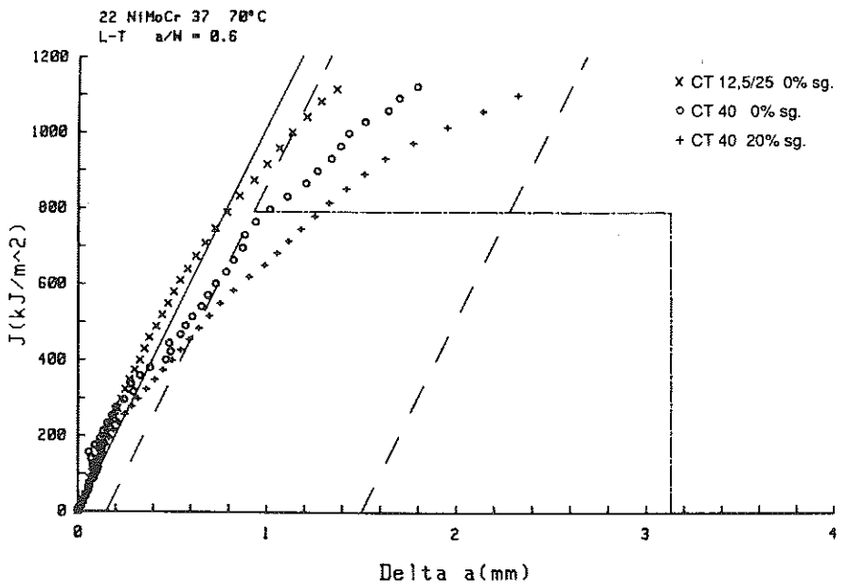

Fig 3 Crack growth resistance curves measured for the material 22 NiMoCr 37 in 70°C

Table 1 Dimensions of the CT specimens

Specimen	*Thickness (mm)*	*Width (mm)*	a/W (−)	*Side-grooves (%)*
AED04	12.5	50	0.60	—
AEF01	40	80	0.61	—
AED02	40	80	0.61	20

The test was stopped at an expected stable crack growth of about 1–2 mm. The final load value was 1.59 MN, the load line displacement as measured from the cylinder was 24.9 mm, and CMOD 2.37 mm. Acoustic emission measurement did not show any signal of crack initiation. For further testing of the acoustic emission technique, the plate was fatigued and the test was repeated with the larger crack size. Comparisons can only be made between the calculation and the experimental results from the first test phase.

The test programme and the analytical and numerical simulations of the tests are thoroughly described in **(4)**.

Description of analytical and numerical part

Analytical calculations and extensive elastic–plastic three-dimensional finite element analyses have been performed for the plate before and after the test. Three CT specimens were chosen from the test series for further analyses. Two of them were smooth specimens with different thickness values and one specimen with 20 percent side-grooves. The dimensions are given in Table 1. The finite element mesh for the side-grooved CT specimen is shown in Fig. 4.

To assess the fracture behaviour of the plate analytically the IWM-VERB program was adopted. Three-dimensional elastic–plastic finite element (FE) calculations were made using the FE program ADINA **(1)** with IWM-CRACK routines **(2)** to simulate stable crack growth.

For the plate test three different finite element calculations have been performed: one analysis with the stationary crack, and two different analyses simulating stable crack growth, using only the lower bound J_R curve obtained from a side-grooved CT specimen and with 'constraint modified' J_R curves.

Normal 20-noded volume elements were used in whole model including the crack tip region which is often modelled with collapsed elements to describe

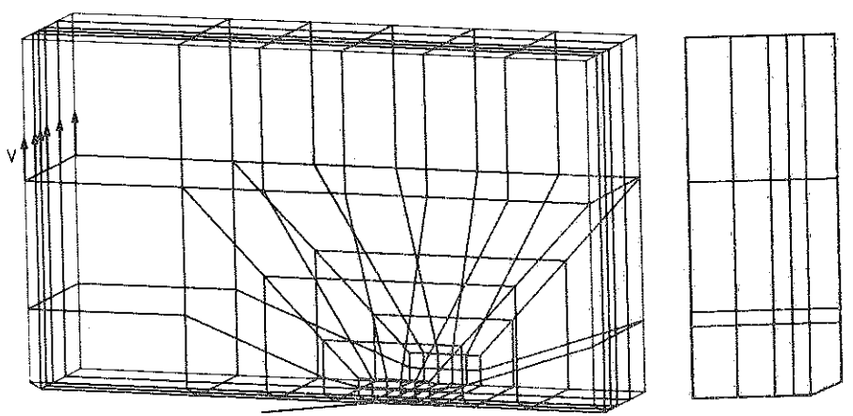

Fig 4 Finite element mesh for the side-grooved CT specimen AED02

the singular strain fields. They cannot describe the blunting of the crack tip which is the most important geometric non-linear effect in the present case. Thus the 'materially non-linear only' (MNLO)-formulation was used.

According to a MNLO calculation the local h value increases continuously when the crack front is approached and it depends thus on the distance from the crack front (see Fig. 5). The present simulations of crack growth are based on the h variation calculated at the Gaussian integration points located nearest to the crack front, at the load level corresponding to initiation. It is assumed, that the h value is not essentially affected by moderate amount of crack growth. CT specimens and the plate are modelled using finite elements of equal size at the crack front. So the h values used for the CT specimens and the plate are consistent.

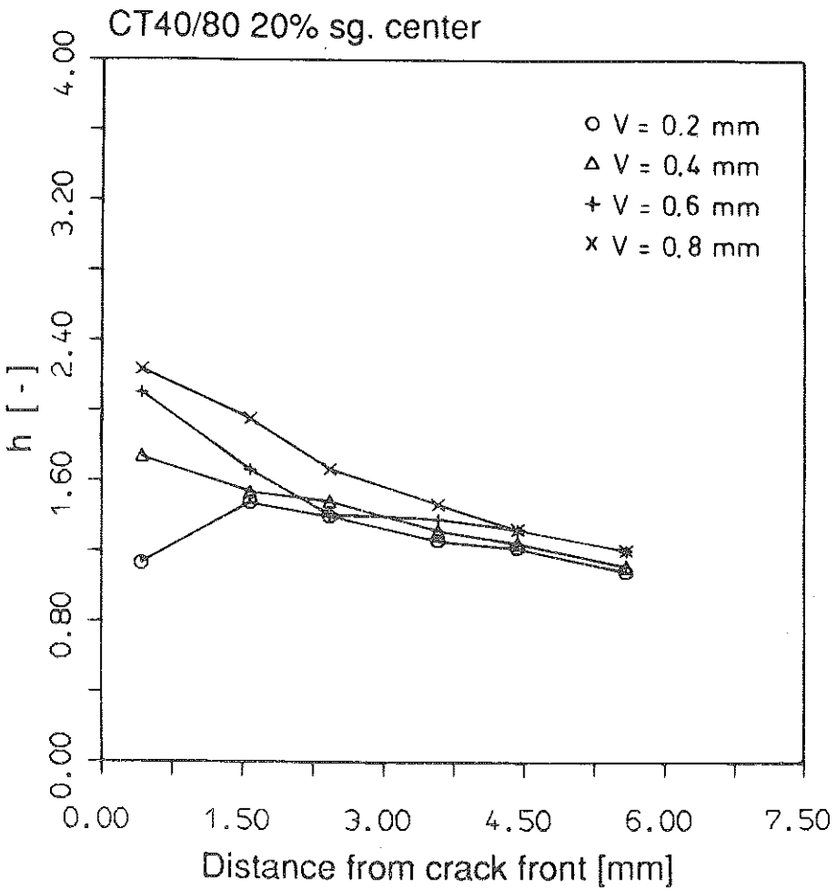

Fig 5 *h* **variation in the ligament of a CT specimen according to a MNLO analysis**

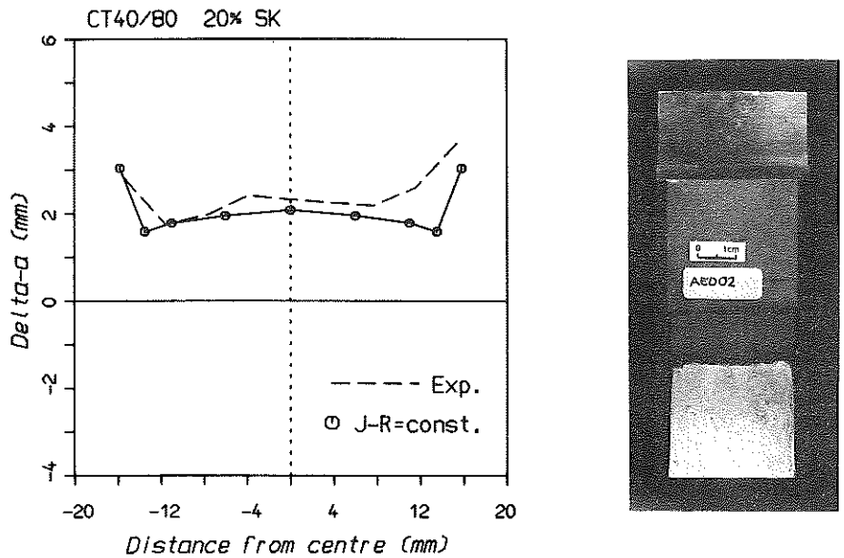

Fig 6 Estimated and measured crack growth in the side-grooved specimen AED02

In a side-grooved CT specimen the local J value and triaxiality of stress state do not vary much along the crack front. Thus it is appropriate to use only one J_R curve in simulating crack growth. This is depicted in Fig. 6 where estimated and measured crack growth are compared for the side-grooved

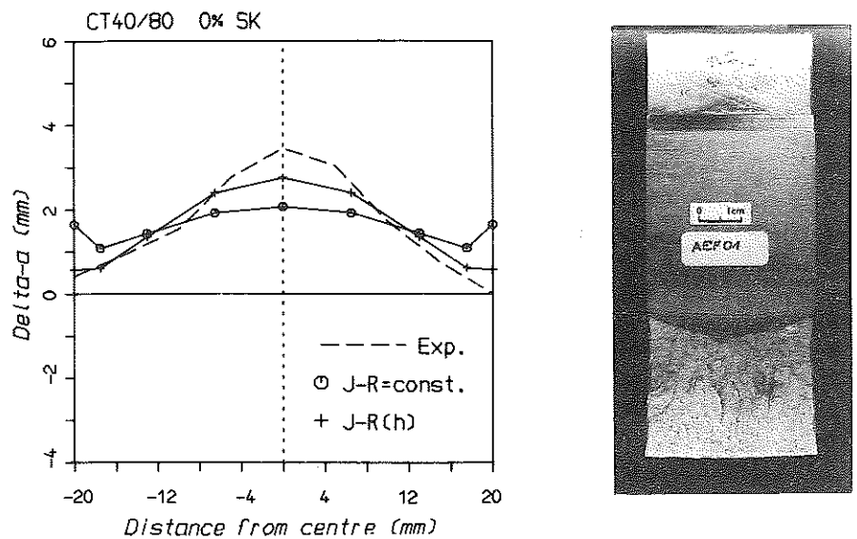

Fig 7 Estimated and measured crack growth in the smooth specimen AEF01

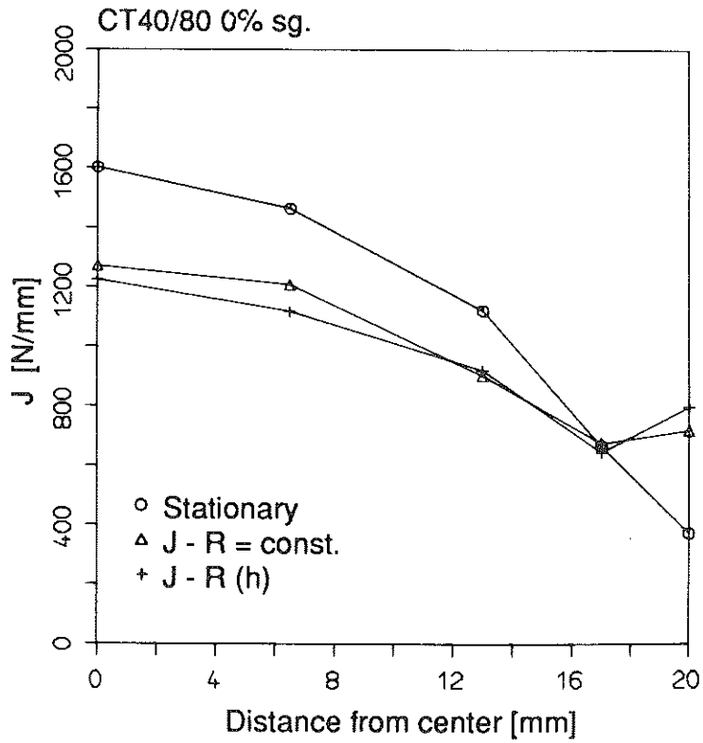

Fig 8 *J* integral distribution along the front of the specimen AEF01 at the end of the test

specimen AED02 at the end of the experiment. The agreement is good even near the bottom of the side-groove which was modelled rather coarsely.

The situation is very different in a smooth specimen. In the analysis for the smooth CT specimens, the effect of the varying constraint was considered. One difficulty was caused by the very low triaxiality level at the outer surface where the stress state is near plane stress. The stress state does thus not correspond there to the average h_m in any of the CT specimens. In a first stage the ASTM blunting line was used as the J_R curve at the outer surface. A comparative analysis was made using only the J_R curve obtained from the thicker smooth specimen AEF01. The results for the specimen AEF01 are compared in Fig. 7. A very clear tunnelling can be seen in the middle of the specimen in the experimental result. None of the simulations was able to reproduce this effect accurately, but a clearly better agreement was achieved when the constraint dependent crack growth resistance was considered. At the outer surface the new model improved the agreement remarkably. In case of the thinner specimen AED04, the situation was more complicated because shear fracture occurred at the outer surfaces.

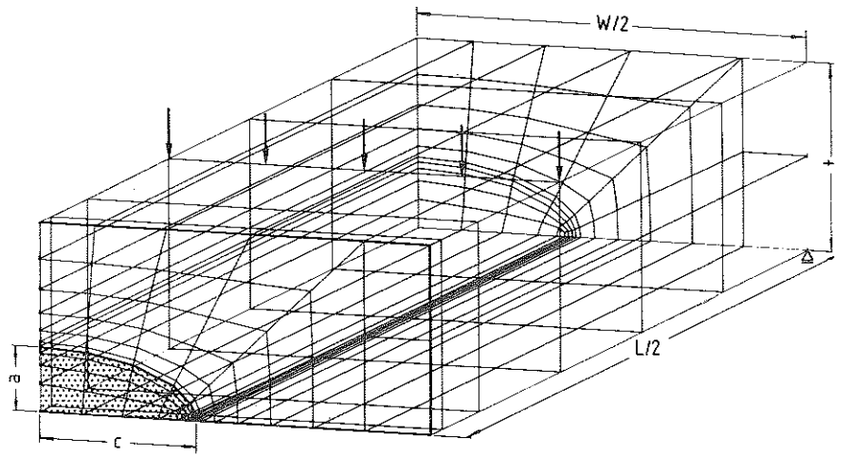

Fig 9 Finite element mesh for the flawed plate

For the smooth specimen AEF01, J variations obtained from a stationary analysis and from the simulations of crack growth were compared. The simulation of crack growth led to a more uniform J distribution compared to the stationary analysis, as shown in Fig. 8. The use of different J_R curves when simulating crack growth did not affect much the local J values.

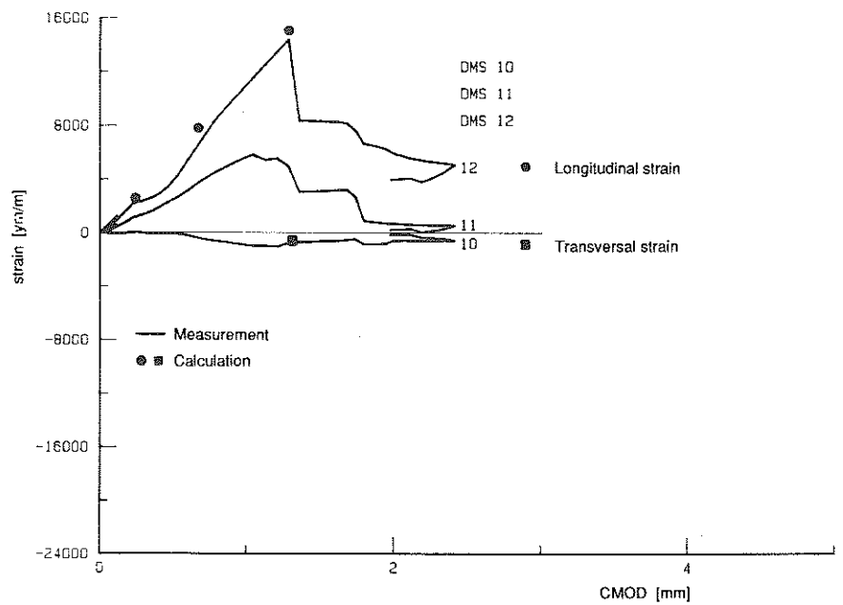

Fig 10 Comparison of measured and calculated strains in the plate near crack end

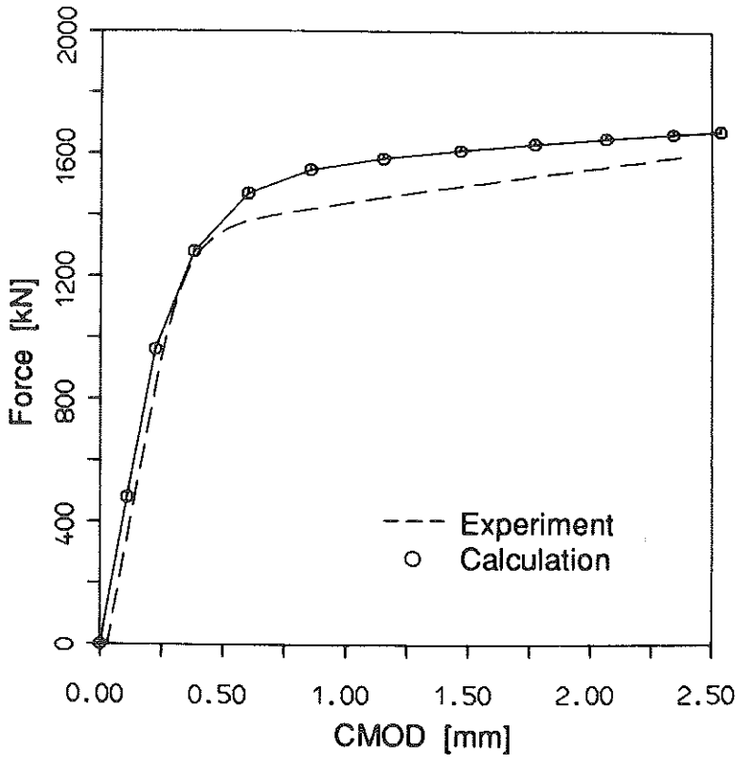

Fig 11 Comparison of measured and calculated load versus load line displacement

Figure 9 represents the finite element model used in the analysis for the plate with the surface flaw. Due to symmetry only one quarter of the plate was modelled. Equal prescribed vertical displacements were imposed along the load line. The size of crack tip elements was the same as in the case of CT specimens.

Calculated and measured strains at the crack side of the plate, near the crack end, are compared in Fig. 10. The agreement between those results was good. As shown in Fig. 11, the calculation somewhat overestimated the load. Main reason for that is probably the rather coarse mesh. At the same CMOD level, the calculated load point displacement was clearly smaller than the measured one (Fig. 12). The discrepancies between load, load point displacement, and CMOD results may be caused by the following reasons.

(1) The displacement was measured directly from the hydraulic cylinder whereas the finite element model did not include the compliance of the loading configuration.
(2) Because the model was rather coarse, especially in the length direction of the plate, it was somewhat too stiff against bending. Additionally, even the nearest Gaussian integration points were therefore a rather large distance from the support lines and thus the model could not consider the local plastic effects there.
(3) Because the MNLO formulation was used, the possible increase in the distance between support lines was not considered. This effect makes the plate more flexible. In the experiment the support rollers were fixed with springs. Their actual displacement was not measured. The finite element calculations indicated, however, that this displacement is at most 5 mm which would affect the load line displacement by less than 1 percent.

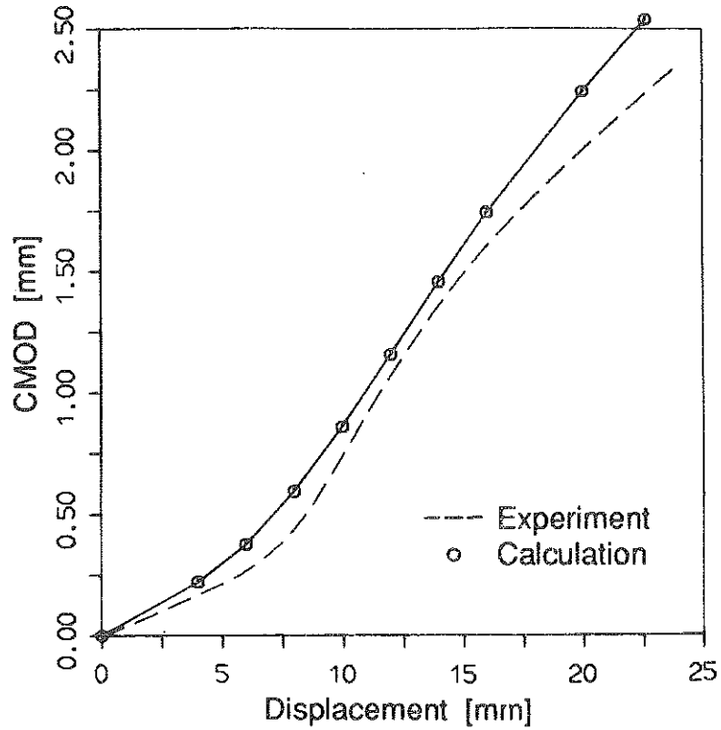

Fig 12 Comparison of measured and calculated CMOD versus load line displacement

Figure 13 shows calculated h variations along the crack front in the plate at different load levels. The constraint parameter had a quite uniform value along the front except very near the outer surface. The value was almost the same as in a side-grooved CT specimen (4). Thus the lower bound J_R curve could be applied in the main part of the crack front. Figure 14 compares J variations at the end of the experiment. As in the case of the smooth CT specimen, both simulations of crack growth led to very similar results as regards to local J values. A stationary analysis yielded higher local J values especially in the

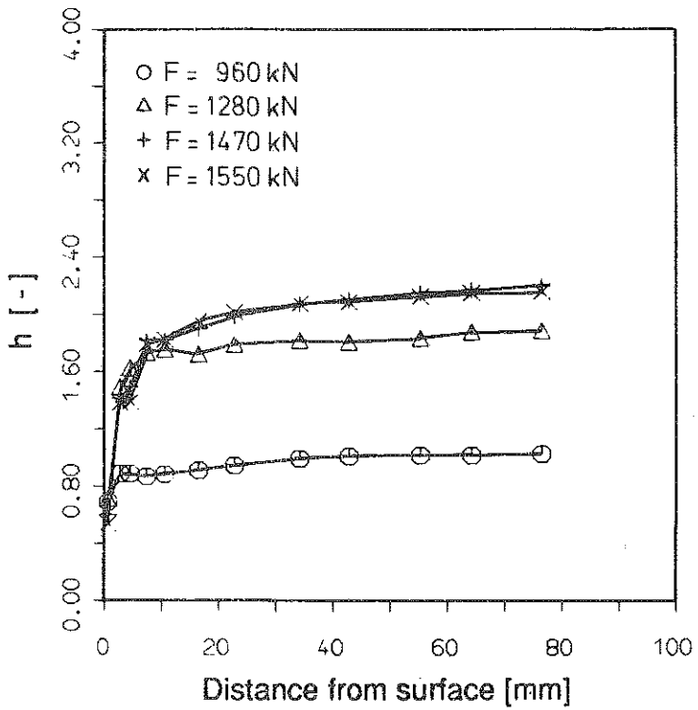

Fig 13 *h* **distribution along crack front in the plate**

middle of the specimen. Thus it may be concluded that a stationary analysis tends to overestimate crack growth at the deepest point of the flaw.

As the final result estimated and measured crack growth are compared in Fig. 15. The amount of stable crack growth was quite small in the experiment. Thus it was difficult to separate apparent crack growth due to blunting from actual stable crack growth. Therefore the crack extension values in Fig. 15 contain the stretch zone. The agreement between calculation and measurement is good. The consideration of the constraint effect improved the result especially near the outer surface.

Table 2 Estimated and measured stable crack growth in the plate. Stretch zone excluded

Method	*Loading parameter*	*Stable crack growth (mm)*
Test	—	0.3
Analytical	Load	0.1
FE	Load	0.3
FE	CMOD	1.1
FE	Displacement	1.4

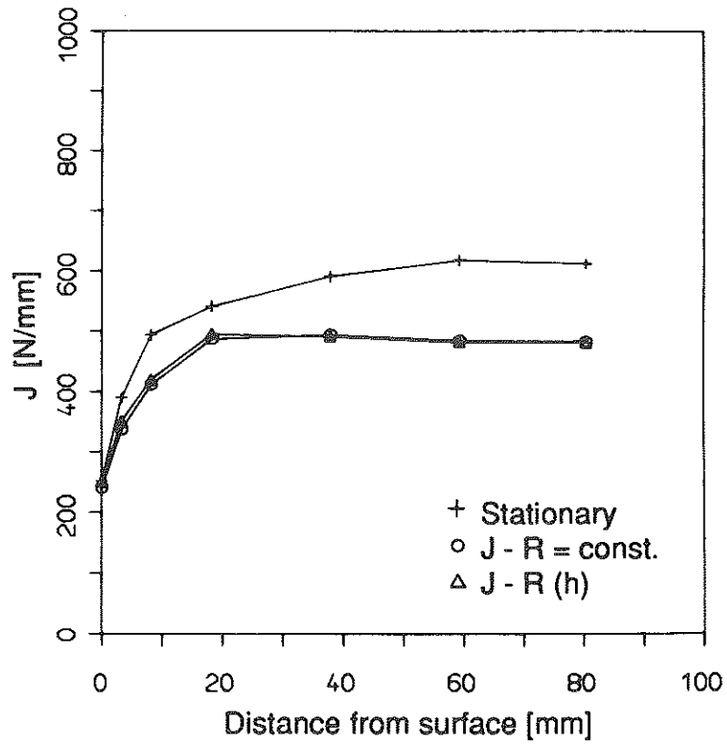

Fig 14 *J* **distribution along crack front in the plate**

Table 2 compares measured stable crack growth (excluding blunting) at the deepest point of the flaw with analytical and numerical results. Different alternative loading parameters were considered. Only the lower bound crack growth resistance curve obtained from a side-grooved CT specimen was used. Due to the discrepancies between load, load point displacement, and CMOD results, which were discussed above, they led to different results. Stable crack growth is underestimated by analytical methods, numerical methods yielded a good agreement when the measured force was used as loading parameter and to an overestimation when CMOD or load line displacement was used.

Summary

The work was aimed as a supplementary link in assuring the applicability of numerical and analytical fracture mechanics methods to the assessment of the behaviour of real structures. Additionally it was aimed as validation of non-destructive examination methods. For this purpose a large flawed plate made of a reactor pressure vessel steel was tested. The loading and temperature at the deepest point of the crack as well as the material behaviour during the test

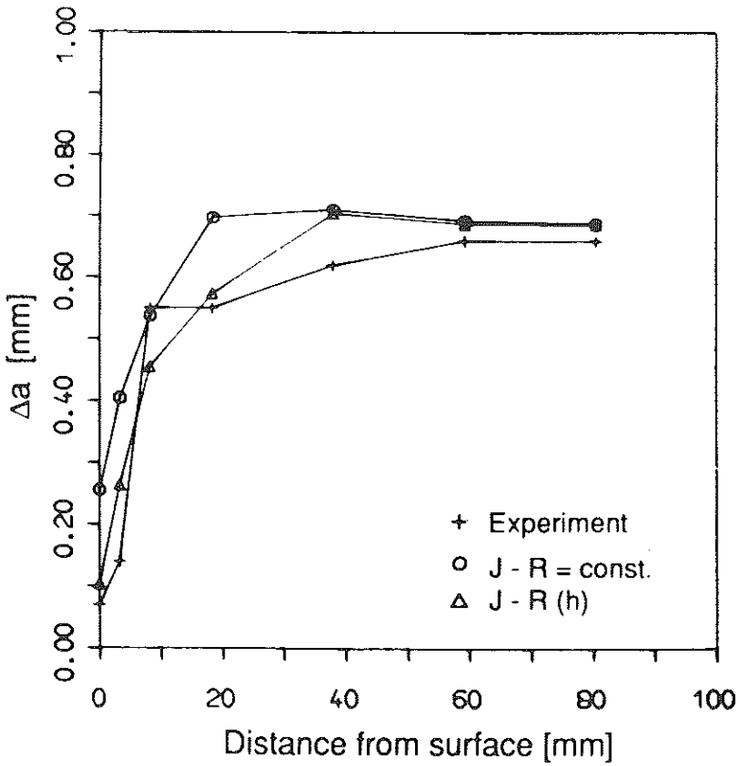

Fig 15 Comparison of measured and estimated crack growth in the plate

were planned to simulate those during a pressurised thermal shock. The material was characterised using stress–strain and crack growth resistance measurements. A number of simulations of stable crack growth in the plate test and tests with CT specimens were made with analytical and numerical methods.

As regards to the plate test, neither the potential measurement method, which has proved very reliable in fracture resistance testing, nor the acoustic emission gave an indication of crack growth. However, some crack growth could be seen in the fracture surface. In calculating stable crack growth, the use of only the lower bound crack growth resistance curve obtained from a side-grooved CT specimen led to different results when different methods were used: to an underestimation by analytical methods, by numerical methods to a good agreement when the measured load was used as loading parameter and to an overestimation when CMOD or load line displacement were used. In the calculation for a side-grooved CT specimen, it was appropriate to use only the lower bound crack growth resistance curve, whereas in the case of smooth CT

specimens it proved to be necessary to consider also the differing local stress state triaxiality.

Good results were achieved in the numerical simulation of local stable crack growth especially when the constraint dependent crack growth resistance was considered. Stationary analyses overestimated local J values, especially in the middle of the specimen, and proved thus to be somewhat conservative.

References

(1) BATHE, K. J. (1980) ADINA, a finite element program for automatic dynamic incremental nonlinear analysis, Report 82 448-1, MIT, Cambridge MA.

(2) IWM-CRACK, a sub-routine package for crack problems, Fraunhofer-Institut für Werkstoffmechanik, Freiburg.

(3) KORDISCH, H., SOMMER, E., and SCHMITT, W. (1989) The influence of triaxiality on stable crack growth, *Nucl. Engng Des.*, **112**, 27–35.

(4) TALJA, H., HODULAK, L., KORDISCH, H., VOSS, B., and KNEE, N. (1988) Durchführung und Analyse eines Laborversuches zur numerischen Simulation des stabilen Rißwachstums, Report V40/88 of the Fraunhofer-Institut für Werkstoffmechanik, Freiburg.

(5) KORDISCH, H., TALJA, H., and NEUBRECH, G. E. (1989) Analysis of initiation and growth of a circumferential crack in the HDR-RPV-cylinder under pressurized thermal shock, SMiRT-10 Post Conference Seminar No. 2, Monterey, CA.